

## Dynamic VLC Navigation System in Crowded Buildings

Manuela Vieira, Manuel Augusto Vieira, Paula Louro,  
Alessandro Fantoni  
ADETC/ISEL/IPL,  
R. Conselheiro Emídio Navarro, 1959-007  
Lisboa, Portugal  
CTS-UNINOVA  
Quinta da Torre, Monte da Caparica, 2829-516,  
Caparica, Portugal

e-mail: [mv@isel.ipl.pt](mailto:mv@isel.ipl.pt), [mv@isel.pt](mailto:mv@isel.pt), [plouro@deetc.isel.pt](mailto:plouro@deetc.isel.pt),  
[afantoni@deetc.isel.ipl.pt](mailto:afantoni@deetc.isel.ipl.pt)

Pedro Vieira  
ADETC/ISEL/IPL,  
R. Conselheiro Emídio Navarro, 1959-007  
Lisboa, Portugal  
Instituto das Telecomunicações  
Instituto Superior Técnico, 1049-001,  
Lisboa, Portugal  
e-mail: [pvieira@deetc.isel.pt](mailto:pvieira@deetc.isel.pt)

**Abstract**— This paper investigates the applicability of an intuitive risk of transmission wayfinding system in public spaces, virtual races, indoor large environments and complex buildings using Visible Light Communication (VLC). Typical scenarios include: finding places, like a particular shop or office, guiding users across different floors, and through elevators and stairs. The system is able to inform the users, in real time, not only of the best route to the desired destination, through a route without clusters of users, but also of crowded places. Data from the sender is encoded, modulated and converted into light signals emitted by the transmitters. Tetra-chromatic white sources are used providing a different data channel for each chip. At the receiver side, the modulated light signal, containing the ID and the 3D geographical position of the transmitter and wayfinding information, is received by a SiC optical sensor with light filtering and demultiplexing properties. Since lighting and wireless data communication is combined, each luminaire for downlink transmission becomes a single cell, in which the optical Access Point (AP) is located in the ceiling and the mobile users are scattered across the overlap discs of each cell, underneath. The light signals emitted by the LEDs are interpreted directly by the receivers of the positioned users. Bidirectional communication is tested. The effect of the location of the Aps is evaluated and a 3D model for the cellular network is analyzed. In order to convert the floorplan to a 3D geometry, a tandem of layers in a orthogonal topology is used, and a 3D localization design, demonstrated by a prototype implementation, is presented. Uplink transmission is implemented, and the 3D best route to navigate through venue is calculated. Buddy wayfinding services are also considered. The results showed that the dynamic VLC navigation system enables to determine the position of a mobile target inside the network, to infer the travel direction along the time, to interact with received information and to optimize the route towards a static or dynamic destination.

**Keywords**- Visible Light Communication; Indoor navigation; Bidirectional Communication; Wayfinding; Optical sensors; Multiplexing/demultiplexing techniques.

### I. INTRODUCTION

This paper is an extended version from the one presented in ALLSENSORS 2021 [1].

Optical wireless communication has been widely studied during the last years in short-range applications. Therefore, communications within personal working/living spaces are highly demanded. The availability of portable communication devices, such as smartphones and tablets increases the demand on mobile wireless connectivity. Several technologies have been investigated to provide wireless connections to the users in indoor and outdoor environments. Nowadays, indoor positioning methods are mainly based on Wi-Fi, Bluetooth, Radio-Frequency Identification (RFID) and Visible Light Communications (VLC) [2][3][4][5]. VLC is a data transmission technology [6] that can easily be employed in indoor environments since it can use the existing LED lighting infrastructure with simple modifications [7][8]. VLC can be regarded as a light based Wi-Fi, i.e., instead of radio waves uses visible light to transmit the data. It presents advantages when compared with the Wi-Fi, namely the invulnerability to the hackers since it does not penetrate through the wall, its high capacity and efficiency. Once lights are essential part of operating rooms, the VLC technology finds applications in a wide variety of fields like: in medical and healthcare, in airlines and aviation, in supermarkets and railway stations, in retail stores, in hidden communication or in Line-of-Sight (LoS) applications as in traffic control, vehicle to vehicle communication or smart street lighting.

The VLC systems use the wavelength range between 380 nm and 780 nm and the LEDs are used as light sources and transmitters. Therefore, the LEDs are twofold by providing illumination, as well as communication. LEDs are incoherent light sources and transmitting information can only be realized by the optical intensity change. Here, the On-OFF keying (OOK) modulation scheme is used. In the sequence, we propose to use modulated visible light, carried out by white tetra-chromatic low cost LEDs. The use of those LEDs provides different data channel for each chip offering the possibility of Wavelength Division Multiplexing (WDM), which enhances the transmission data rate. At the receiver side, the modulated light signal is received by a SiC photodetector, based on a tandem a-

SiC:H/a-Si:H pin/pin structure, which presents light filtering and demultiplexing properties decoding the received information [9] [10]. Here, when different visible signals are encoded in the same optical transmission path, the device multiplexes the different optical channels, performs different filtering processes (amplification, switching, and wavelength conversion) and finally decodes the encoded signals recovering the transmitted information.

Research is still necessary to design LED arrangements that can optimize communication performance while meeting the illumination constraints for a variety of large indoor layouts. Visible light can be used as an ID system in different places such as buildings and subways and can be employed for identifying the room number and its building. The main idea is to divide the space into spatial beams originating from the different ID light sources, and identify each beam with a unique timed sequence of light signals. Fine-grained indoor localization can enable several applications; in airports, supermarkets and shopping malls. Exact location of products can greatly improve the customer's shopping experience and enable customer analytics and marketing [11]. The signboards, based on arrays of LEDs, positioned in strategic directions to broadcast the information [12], are modulated acting as down- and up-link channels in the bidirectional communication.

In this paper, a LED-supported positioning and navigation VLC system is proposed. After the Introduction, in Section II, a VLC scenario for large environments is established, the emitters and receivers are characterized and the communication protocol presented. In Section III, the main experimental results are presented, the effect of the location of the optical Access Points (Aps) is evaluated and a model for the different cellular networks is analysed. Square and hexagon mesh are tested, and a 2D localization design, demonstrated by a prototype implementation, is presented. Uplink transmission is implemented and the 2D best route to navigate through venue calculated. In Section IV, the conclusions are drawn showing that the system makes possible to determine the position of a mobile target inside the network, to infer the travel direction along the time and to interact with information received.

## II. VLC NETWORK

In the follow, the VLC network is described.

### A. Self-localization

Self-localization is a fundamental issue since the person must be able to estimate its position and orientation (pose) within a map of the environment it is navigating. We consider the path to be a geometric representation of a plan to move from a start pose to a goal pose. Let us consider a person navigating in a 2D environment (Figure 1). Its non-omnidirectional configuration is defined by position  $(x, y)$  and orientation angle  $\delta$ , with respect to the coordinate axes.

$q(t) = [x(t), y(t), \delta(t)]$  denotes its pose at time  $t$ , in a global reference frame. In cooperative positioning systems, persons are divided into two groups, the stationary persons and the moving persons. Let us consider that  $q_i(t, t')$  represents the pose of person  $i$  at time  $t'$  relative to the pose of the same person at time  $t$  and  $q_{ij}(t)$  denotes the pose of person  $j$  relative to the pose of person  $i$  at time  $t$ .  $q_i(t, t')$  is null for people standing still and non-zero if they move. These three types of information  $q_i(t)$ ,  $q_i(t, t')$  and  $q_{ij}(t)$  compose the basic elements of a pose graph for multi-person cooperative localization.

Person-to-person spread to be the most common form of transmission of COVID-19, occurring mainly among people who are within 2m of each other for a prolonged period of time. This means people should stay the recommended distance apart from others. It also means people should avoid gathering in groups, crowded places and mass gatherings. So, in crowded building the routes to a specific place should avoid those regions. We consider that the risk of transmission exists if  $q_{ij}(t)$  is less than 2 m. The system has to alert the users to stay away from those regions and to plan the better route to the desired wayfinding services. To estimate each person track the pure pursuit approach [13], [14] is used. The principle took into account the curvature required for the mobile receiver to steer from its current position ( $t_1$ ) to its intended position ( $t_2$ ). By specifying a look-ahead distance, it defines the radius of an imaginary circle. Finally, a control algorithm chooses a steering angle in relation to this circle. Then, this allows to iteratively construct the intermediate arcs between itself and its goal position as it moved, thus, obtaining the required trajectory for it to reach its objective position. To avoid the risk of transmission, in the same frame of time and in known crowded regions,  $q_{ij}(t)$  is estimated and the steering angle readjusted.

### B. Virtual scenario and Architecture

When we are looking for the shortest route to a place, we want to be guided on a direct, shortest path to our destination. Advances in wayfinding responds to our need to establish markers and identify patterns by creating spatial relationships between users and areas. Directional aids remain in force, but there is now a digital framework that goes beyond providing basic information. This expansion has encouraged the rise of multi-device connectivity that can tell users where they are (current point), where they need to be (goal point) and what they need to do to get there (path).

Interaction between planning, control, and localization is important. The localization (Where am I?) senses the environment and computes the user position, the planning (Where am I going?) computes the route to follow from the position and the control (How do I get there?) moves the user in order to follow the route. A destination can be targeted by user request to the Central Manager (CM).

The simulated scenario is an airport. Here, the traveler, equipped with a receiver, navigates from outdoor to indoor. It sends a request message to find the right track and, in the available time, he adds customized points of interest and halls to boarding. During his path, the passenger is advised how to reach its destination and the possibility to use location based advertising services. The requested information is sent by the emitters at the ceiling to its receiver. In Figure 1, the proposed architecture and scenario are illustrated.

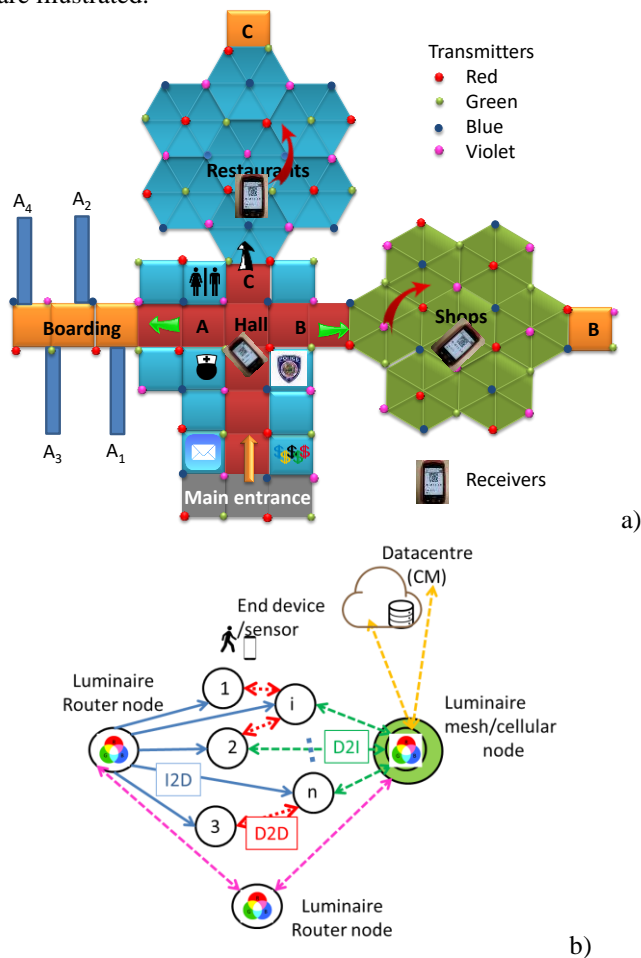


Figure 1 a) Optical infrastructure and indoor layout. b) Mesh and cellular hybrid architecture

Two topologies were considered: the square for the main hall and the hexagonal for the marketing zones (Figure 1a). Data from the infrastructure is encoded, modulated and converted into light signals emitted by the transmitters. Tetra-chromatic (Red, Green, Blue, Violet) white sources are used, providing a different data channel for each chip. At the receiver side, the modulated light signal, containing the ID and the 2D geographical position of the transmitter and wayfinding information, is received by a SiC photodetector with light filtering and demultiplexing properties. To synchronize the signals from multiple LEDs,

the transmitters use different IDs, allowing the signal to be reconstructed at the receiver.

We propose a mesh cellular hybrid structure to create a gateway-less system without any external gateways needed. We propose this network configuration since it is wireless and ad-hoc. It spans all devices, is wire free, demonstrate resiliency to physical obstructions and adapt to changes in the transmission medium. Therefore, a mesh network is a good fit because it dynamically reconfigures itself and grows to the size of any installation. It is also a secure and trustworthy network [15]. As illustrated in Figure 1b, the luminaires, in this architecture, are equipped with one of two types of nodes: A “mesh” controller that connects with other nodes in its vicinity. These controllers can forward messages to other devices (I2D) in the mesh, effectively acting like routers nodes in the network. A “mesh/cellular” hybrid controller equipped with a modem provides IP base connectivity to the central manager services (CM). These nodes act as border-router and can be used for edge computing. Under this architecture, the short-range mesh network purpose is twofold: enable edge computing and device-to-cloud communication, by ensuring a secure communication from a luminaire controller to the edge computer or datacenter (I2CM), through a neighbor luminaire controller with an active cellular connection; and enable peer-to-peer communication (I2IP), to exchange information between smart devices.

Building a geometry model of interiors of buildings is complex since the interior structure has to be seen as an aggregation of several different types of objects (rooms, stairs, etc.) with different shapes. In the proposed architecture the logical model is easier since represents each room/crossing/exit with a node (Figure 1a), and a path as the links between nodes. The user positions can be represented as  $P(x, y)$  by providing the horizontal positions  $(x, y)$ . The indoor route throughout the building is presented to the user by a responding message transmitted by the ceiling luminaires that work also either as router or mesh/cellular nodes (Figure 1b). With this request/response concept, the generated landmark-based instructions help the user to unambiguously identify the correct decision point where a change of direction (pose) is needed, as well as offer information for the user to confirm that he/she is on the right way.

### III. VLC LINK MODELS

#### A. VLC dynamic navigation system (position and route control)

To support people’s wayfinding activities in unfamiliar indoor environments, a method able to generate ceiling landmark route instructions using VLC is proposed. The dynamic navigation system is composed of several transmitters (LEDs ceiling luminaries), which send the map information and path messages required to wayfinding. A mobile optical receiver, using joint transmission, extracts

user location to perform positioning and, concomitantly, the transmitted data from each transmitter. To synchronize the signals from multiple LEDs, the transmitters use different ID's, such that the signal is constructively at the receiver. Bidirectional communication between the emitters and the receivers is available in strategic optical access point (Li-Fi zone). The block diagram of the VLC system is presented in Figure 2.

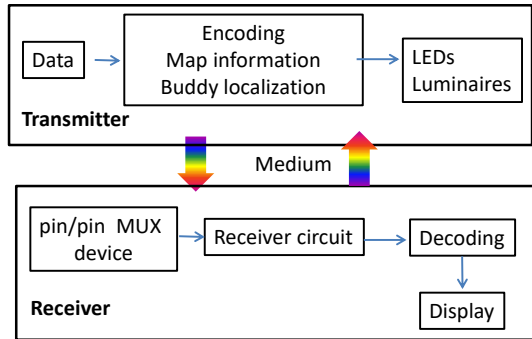


Figure 2. VLC block diagram of the VLC system.

The system is composed by the transmitter and the receiver modules located, respectively, at the infrastructures and at the mobile users. The VLC receiver, at the reception end of the communication link, is responsible to extract the data from the modulated light beam. It transforms the light signal into an electrical signal that is subsequently decoded to extract the transmitted information.

The principal components of the VLC system are the LEDs, which act as the communication sources and the SiC WDM devices that serve as receiving elements. Data from the sender is converted into an intermediate data representation, byte format, and converted into light signals emitted by the transmitter module. The data bit stream is input to a modulator where an ON-OFF KEYING (OOK) modulation is utilized. Here, a bit one is represented by an optical pulse that occupies the entire bit duration, while a bit zero is represented by the absence of an optical pulse.

The light signal is received by the WDM photodetector that detects the on/off states of the LEDs, generates a binary sequence of the received signals and convert data into the original format. The LEDs emit light when the energy levels change in the semiconductor diode. The wavelength depends on the semiconductor material used to form the LED chip. For data transmission, commercially available polychromatic white LEDs were used at the nodes of the network. On each node only one chip is modulated for data transmission and carries useful information while the others are only supplied with DC to maintain white colour illumination. Red (R; 626 nm), Green (G; 530 nm), Blue (B; 470 nm) and violet (V; 390 nm) LEDs, are used [16][17]. Since lighting and wireless data communication is combined, each luminaire for downlink transmission becomes a single cell, in which the optical access point (AP)

is located in the ceiling and the mobile users are scattered within the overlap discs of each cells underneath.

LEDs are modeled as Lambertian sources where the luminance is distributed uniformly in all directions, whereas the luminous intensity is different in all directions. The luminous intensity for a Lambertian source is given by Equation (1) [18]:

$$I(\phi) = I_N \cos(\phi)^m \quad (1)$$

Where  $m$  is the order derived from a Lambertian pattern,  $I_N$  is the maximum luminous intensity in the axial direction and  $\phi$  is the angle of irradiance. The Lambertian order  $m$  is given by:

$$m = \frac{\ln(2)}{\ln(\cos(\phi_{1/2}))} \quad (2)$$

For the proposed system, the commercial white LEDs were designed for illumination purposes, exhibiting a wide half intensity angle ( $\phi_{1/2}$ ) of  $60^\circ$ . Thus, the Lambertian order  $m$  is 1.

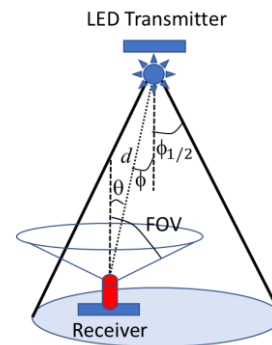


Figure 3. Geometry of the relative position of the transmitter and receiver units.

The light signal is received by the WDM photodetector that detects the on/off states of the LEDs, generates a binary sequence of the received signals and convert data into the original format. For simplicity we will consider a line of sight (LoS) connection for both VLC links, which corresponds to the existence of straight visibility between the transmitter and the receiver. In Figure 3, it is plotted the geometry of the transmitter and receiver relative position, with emphasis to the main parameters used for characterization of the LED source and the photodiode receiver (angles of irradiance and illumination, transmitter's semi-angle at half-power and field of view). The Lambertian model is used for LED light distribution and MatLab simulations are used to infer the signal coverage of the LED in the illuminated indoors space [19] [20].

The VLC photosensitive receiver is a two terminal double PIN photodetector based on a multilayer heterostructure, p-i'(a-SiC:H)-n/p-i(a-Si:H)-n. Two transparent front and back contacts are used [9]. The device

presents high sensitivity and linear response in the visible range generating at the terminals a proportional photocurrent. It fast response enables the possibility of high speed communications. Modulated light supplied by the polychromatic LEDs is used for data transmission. The signals are encoded into colours intensities emitted by red, green, blue and violet LEDs. The generated photocurrent is processed using a transimpedance circuit and the proportional voltage is processed, by using signal conditioning techniques (adaptive bandpass filtering and amplification, triggering and demultiplexing), until the data signal is reconstructed at the data processing unit (digital conversion, decoding and decision) [16].

**B. Large Environments emitters and receivers**

Lighting in large environments is designed to illuminate the entire space in a uniform way. Ceiling plans for the LED array layout is shown in Figure 4.

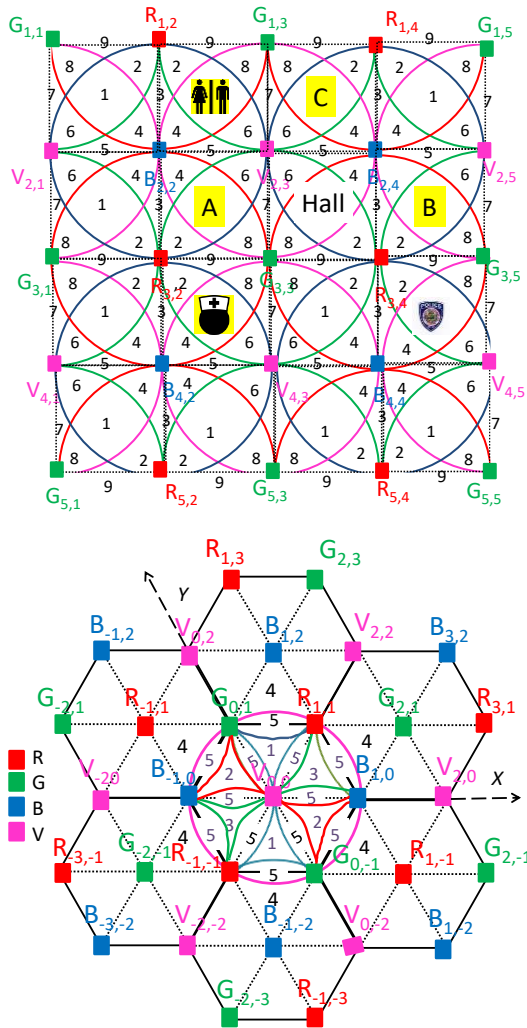


Figure 4. Illustration of the optical scenarios (RGBV >modulated LEDs spots). Cellular topologies: a) Clusters of cells in square topology . b) Clusters of cell in hexagonal topology.

Two topologies considered: the square, (Figure 4a) and the hexagonal (Figure 4b). In the square topology the cells have squares shapes while in the hexagonal one they are distributed to form a hexagonal shaped constellation. To receive the information from several transmitters, the receiver must be positioned where the circles from each transmitter overlap, producing at the receiver, a multiplexed (MUX) signal that, after demultiplexing, acts twofold as a positioning system and a data transmitter. In both, the grid sizes were chosen to avoid overlap in the receiver from adjacent grid points. The coverage map for a square unit cell is displayed in Figure 5. All the values were converted to decibel.

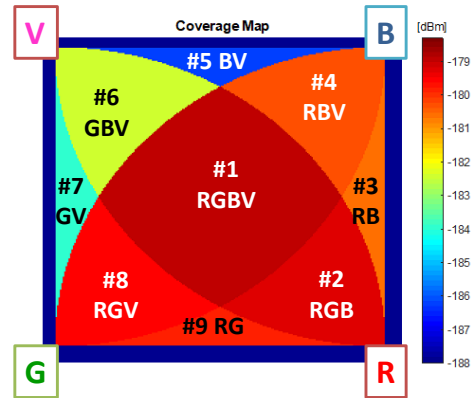


Figure 5. Illustration of the coverage map in a square unit cell.

Friis’ transmission equation is frequently used to calculate the maximum range by which a wireless link can operate. The coverage map is obtained by calculating the link budget from the Friis Transmission Equation [21]. The Friis transmission equation relates the received power ( $P_R$ ) to the transmitted power ( $P_E$ ), path loss distance ( $L_R$ ), and gains from the emitter ( $G_E$ ) and receiver ( $G_R$ ) in a free-space communication link.

$$P_R [dBm] = P_E [dBm] + G_E [dB] + G_R [dB] - L_R [dB] \tag{3}$$

Taking into account Figure 3, the path loss distance and the emitter gain will be given by:

$$L_R [dB] = 22 + 20 \ln \frac{d}{\lambda} \tag{4}$$

$$G_E [dB] = \frac{(m + 1)A}{2\pi d_{E-R}^2} I(\theta) \cos(\theta) \tag{5}$$

With A the area of the photodetector and  $d_{E,R}$  the distance between each transmitter and every point on the receiver plane.



The receptors act as active filters [9] [16]. Due to their filtering properties the gains are strongly dependent on the wavelength of the pulsed LEDs. Gains of 5, 4, 1.7 and 0.8 were used, respectively, for the R, G, B and V LEDs.

The coverage map, Figure 5, was obtained by calculating the link budget using the Equation (3). The input parameters are displayed in Table 1. All the values were converted to decibel.

TABLE 1. LINK BUDGET INPUT.

Variable	Value			
	Red LED	Green LED	Blue LED	Violet LED
$I_N(\text{mcd})$	730	650	800	900
$G_E(\text{dB})$	Equation (5)			
$G_R$	5	4	1.7	0.8
$L_R(\text{dB})$	Eq. (4)			

Users in different locations are served simultaneously by the same transmitter leading to a fine grained implementation. Due to the overlapping coverage area of adjacent Aps joint transmission exists. In Table II, and for both topologies, the overlap regions below each AP (footprints) are displayed. Results show that the received power in each cell depends on the receiver position. Nine separated levels were found, in the square topology, and correspond to the nine possible combinations of the pulsed LEDs framed at corners of the unit cell (Figure 4a). The same occurs in the hexagonal topology (Figure 4b) where five different levels are detected.

TABLE 2. FINE-GRAINED TOPOLOGIES: FOOTPRINT REGIONS.

Footprint regions	Square topology	Hexagonal topology
#1	RGBV	RGV
#2	RGB	GBV
#3	RB	RBV
#4	RBV	RGB
#5	BV	RGBV
#6	GBV	-
#7	GV	-
#8	RGV	-
#9	RG	-

In both topologies, each node,  $X_{i,j}$ , carries its own color, X, (RGBV) as well as its ID position in the network (i,j). The overlap regions (footprints) are pointed out in Figure 4 and reported in Table 1. The device receives multiple signals, finds the centroid of the received coordinates and stores it as the reference point position (# in Figure 5).

C. Modulation technique

An on-off keying (OOK) modulation scheme was used providing a good trade-off between system performance and implementation complexity.

The OOK transmits data by sequentially turning on and off the LED providing digital dimming support. To create a communication protocol to ensure the required system performance and overcome the technology constraints, a 32 bits data frame was designed. Three control fields, one for synchronism (Sync.) and two for the identification of the cell (ID) begin each frame. This sequence is followed by a fourth block that is for the payload, as it is shown, for both topologies, in Figure 6. A stop bit is used at the end of each frame.

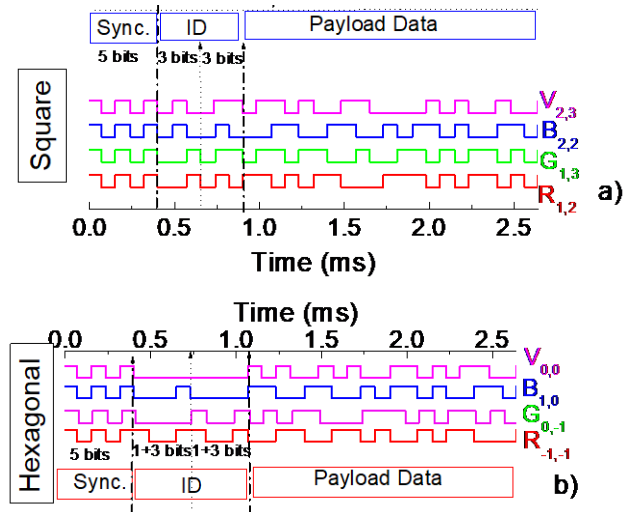


Figure 6. Data frame structure. Representation one encoded message, in a time slot from the array in the network: a) Square topology;  $R_{1,2}$ ;  $G_{1,3}$ ;  $B_{2,2}$  and  $V_{2,3}$  are the transmitted node packet. B) Hexagonal topology;  $R_{-1,-1}$ ;  $G_{0,-1}$ ;  $B_{1,0}$  and  $V_{0,0}$  are the transmitted node packet.

The first five bits in the frame are used for time synchronization. The same synchronization header [10101], in an ON-OFF pattern, is imposed simultaneously to all emitters. Each colour signal (RGBV) carries its own ID-BIT, so, the next bits give the coordinates of the emitter inside the array ( $X_{i,j}$ ). Cell's IDs are encoded using a binary representation for the decimal number. In the square topology (Figure 4a) six bits are used: the first three for the binary code of the line and the other three for the column. In the hexagonal topology, 60° Cartesian coordinates were applied (Figure 4b). Here, an extra bit was added at the

beginning of the binary code to represent the number's sign: setting that bit to 0 is for a positive number, and setting it to 1 is for a negative number. The remaining bits in the number indicate the absolute value. So, the next eight bits (ID) are assigned, respectively, to the  $x$  and  $y$  coordinate ( $I, j$ ) of the emitter in the array (Figure 3b). For both, the last bits, in the frame, are reserved for the message send by the  $X_{ij}$  node (payload data). With this information, the method will give an unique answer, *i.e.*, the location of the receiver in the array ( $X_{i,j}$ ) and the broadcast information.

Results show that in the square network  $R_{1,2}$ ,  $G_{1,3}$ ,  $B_{2,2}$  and  $V_{2,3}$  are the transmitted node packets, in a time slot, from the unit cell where the restrooms are located (Figure 4a). In the hexagonal network, the nodes  $R_{-1,-1}$ ,  $G_{0,-1}$ ,  $B_{1,0}$  and  $V_{0,0}$ , at the first ring of the restaurant zone (Figure 4b) are the transmitters.

#### IV. EXPERIMENTAL RESULTS AND DISCUSSION

In this section, the main results are presented and discussed.

##### A. Decoding

In a data frame, the MUX signal at the receiver, due to the joint transmission of four R, G, B and V optical signals, is presented in Figure 7. The data acquisition was obtained under environment light. On the top, the bit sequence used to drive the LEDs is displayed. This sequence allows all the *on/off* sixteen possible combinations of the four input channels ( $2^4$ ).

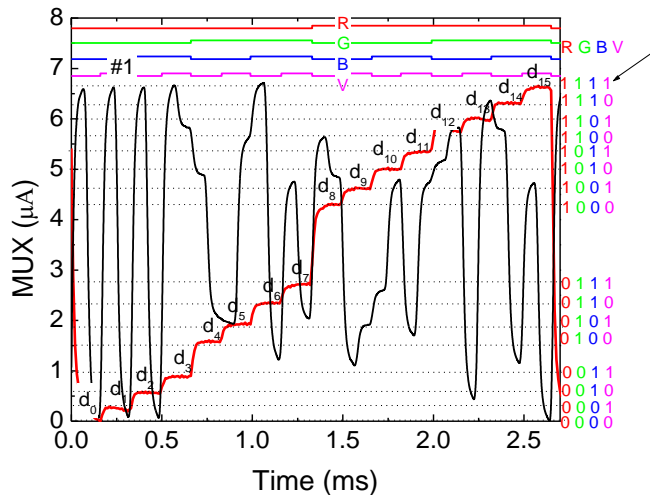


Figure 7. MUX signal of the calibrated cell. On the top the transmitted channels packets [R, G, B, V] are depicted. A received MUX signal is also superimposed to exemplify the decoding process.

Results show that the code signal presents as much separated levels as the *on/off* possible combinations of the input channels, allowing decoding the transmitted information [16]. All the ordered levels ( $d_0$ - $d_{15}$ ) are pointed out at the correspondent levels, and are displayed as

horizontal dotted lines. In the right hand side the match between MUX levels and the 4 bits binary code assigned to each level is shown. For demonstration of the decoding technique, a signal received, in the same frame of time, when the receiver is in the main the hall (Figure 4a) underneath position #1, is also added. Comparing the calibrated levels ( $d_1$ - $d_{15}$ ) with the different assigned 4-digit binary code, the decoding is straightforward.

After decoding each input channel, and taking into account the frame structure (Figure 6), the position of the receiver and its ID in the network is revealed [22] [23]. The footprint position comes directly from the synchronism block, where all the received channels are simultaneously *on* or *off*. For instance, in any footprint #1 the maximum amplitude detected (see arrow) corresponds to the binary word [1111], meaning that the received information comes from the overlap of the four input channels.

##### B. Positioning

In Figure 8, for the same frame time and in three successive instants ( $t_1$ ,  $t_2$ ,  $t_3$ ), the received MUX signals, when the receiver is in the main hall and moves from #5 to #9, through #1 (Figure 4a), confirm the decoding process.

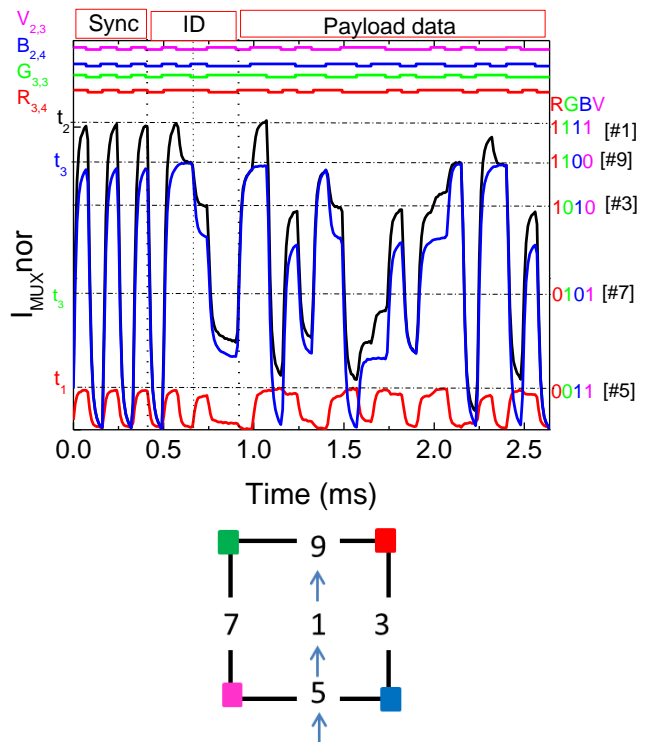


Figure 8. Fine-grained indoor localization and navigation in successive instants ( $t_1$ ,  $t_2$  and  $t_3$ ): MUX/DEMUX signals in a point-to-point path across the main hall ( $\#5 \rightarrow \#1 \rightarrow \#9$ ) at the. On the top the complete transmitted channels packets [R, G, B, V] are decoded.

Decoding, when the four channels overlap (#1), is set on the top of the figure to direct into the packet sent by each

node. The footprint position comes directly from the synchronism block. For instance, if the maximum amplitude detected corresponds to the binary word [0011], it means that it has only received the overlap transmission from the blue and the violet channels (footprint #5). In the right side of the figure the levels ascribed to #1, #3, #5 and #9 are point it out.

Each decoded message carries, also, the transmitter's node address. So, the next block of six bits, in the square topology (or eight in the hexagonal one), gives the ID of the received node. In Figure 8, in position #5 the network location of the transmitters are  $B_{2,4}$  [010;100] and  $V_{2,3}$  [010;011] and while in #1 the assigned transmitters are  $R_{3,4}$ ,  $G_{3,3}$ ,  $B_{2,4}$  and  $V_{2,3}$ . The last block is reserved for the transmission of the advertising (Payload data). The stop bit (0) is used always at the end of each frame.

C. Point-to-point Route

To compute the point-to-point along a path, we need the data along the path. The input of the aided navigation system is the coded MUX signal, and the output is the system state decoded at each time step ( $\Delta t$ ). As a proof of concept, in the lab, a navigation data bit transition was tested by moving the receiver along known pattern path.

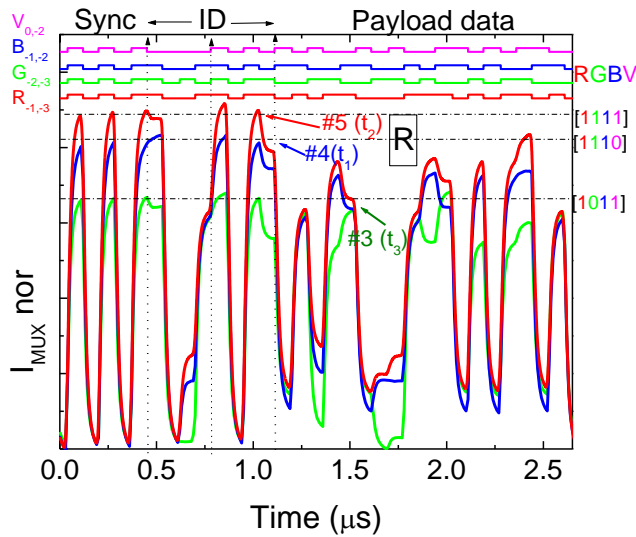


Figure 9 Fine-grained indoor localization and navigation in successive instants instants ( $t_1$ ,  $t_2$  and  $t_3$ ). Signal acquisition through the restaurants area (R). On the top the transmitted channels packets are decoded [R, G, B, V].

In this example (Figure 8) at  $t_1$  the user enters the hall by line #5, it goes to position #1 at  $t_2$  and it chooses the boarding terminal C (#5) at  $t_3$ . Results show that, as the receiver moves between generated point regions, the received information pattern changes. Between two consecutive data sets, there is a navigation data bit transition (channel is missing or added). We observe that when the receiver moves from #1 to #9 (Figure 8) two different ID channels are missing ( $B_{2,4}$  and  $V_{2,3}$ ). Here, the 4-bynary bit code has changed from [1111] to [1100].

In Figure 9, a path across the hexagonal topology was also tested. Here, the receiver enters the restaurants area (#4> #5> #3).

Main results from both topologies show that fine grained localization is achieved by detecting the wavelengths of the received channels in each region. The location and path of a mobile receiver was obtained based on the LED-based navigation system. In an orthogonal layout (hall), the square topology is the best. It allows crossroads and the client can walk easily in the horizontal, vertical or both directions. In concentric layouts, to fill all the space with hexagon presents advantages (restaurants, and shops areas). Here, the client can move around and walk between the different rings toward the outside region.

D. Bidirectional Communication

The VLC is a wireless broadband technology. It provides multiuser with simultaneous access communication. All the nodes communicate with each other through a centralized controller and the signal is used to establish a point-to-point link between the transmitters and the receiver.

Bidirectional communication between VLC emitters and receivers at a handheld device can be established through a control manager linked to a signboard. Each ceiling lamp broadcasts a message with its ID and useful information which is received and processed by the receiver. Using a white polychromatic LED as optical source for uplink, the receptor sends to the local controller a "request" message with its location (ID) and adds its needs for the available time (Payload data). For route coordination, the local controller emitter sends the downlink "response" message. In Figure 10, the MUX signal assigned to a "request" and a "response" message are displayed. In the top, the decoded information is presented. In the right side, the match between the MUX signal and the 4-binary code is pointed out.

Here, in a time slot, the traveler, in position #3 ( $R_{3,2}$ ,  $B_{2,2}$ ), sends to the central controller the message "request" in order to add the points of interest (boarding or the right track). After that it is advised, through a "response" message, that the request was received, how to reach its destination in time and how to use location based services.



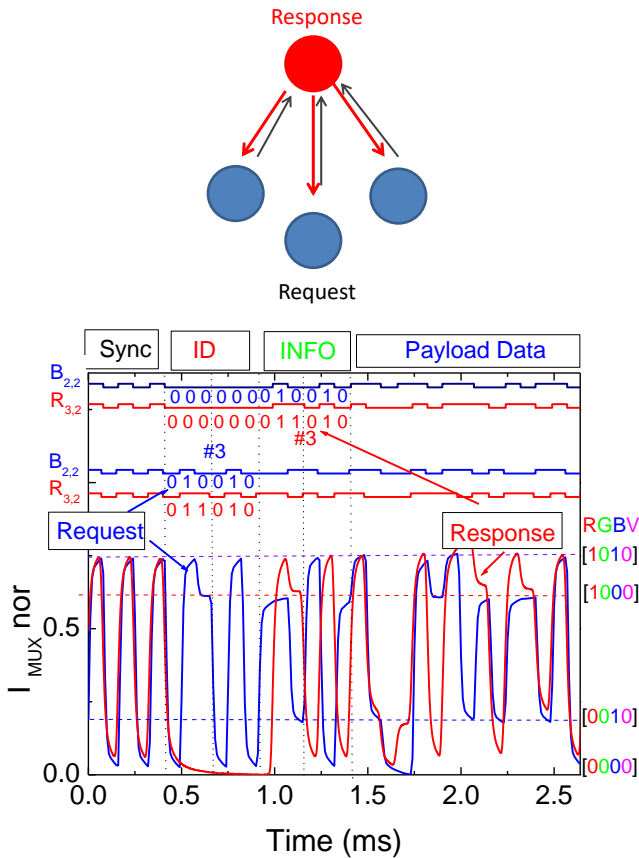


Figure 10. Bidirectional communication: MUX/DEMUX signals assigned to a “request” and a “response” message. On the top the transmitted channels packets  $[X_{i,j}]$  are decoded.

In bidirectional VLC transmission we use different codes in the frame structure for uplink and downlink. Taking into account the frame structure (Figure 6), results show that the codification of both signals is synchronized (Sync). The “request” message includes the complete address of the traveller (Sync+ID) and the help need (Payload Data). In the “response” message the block (ID), in a pattern [000000], means that a response message, from the local manager, is being sent. The next block (6 bits) identifies the address (INFO) for which the message is intended and finally in the last block appears the requested information (Payload Data). Here, the emitter controller [000000] responds to a request of a passenger located in position # 3 ( $R_{3,2}$ ,  $B_{2,2}$ ) and sends back the requested information.

E. Multi-person cooperative localization

An unforeseen pandemic is facing the world caused by a corona virus known as SARS-CoV-2. Transmission of the coronavirus is possible indoors, especially when people spend extended periods in crowded and poorly ventilated rooms [ 24 ]. The widely accepted main transmission mechanism is through droplet borne pathways.

Person-to-person spread to be the most common form of transmission of COVID-19, occurring mainly among people who are within 2m of each other for a prolonged period of time. This means people should stay the recommended distance apart from others. It also means people should avoid gathering in groups, crowded places and mass gatherings. So, in crowded building the routes to a specific place should avoid those regions. We consider that the risk of transmission exists if the distance between two users is less than 2 m. The system has to alert the users to stay away from those regions and to plan the better route to the desired wayfinding services.

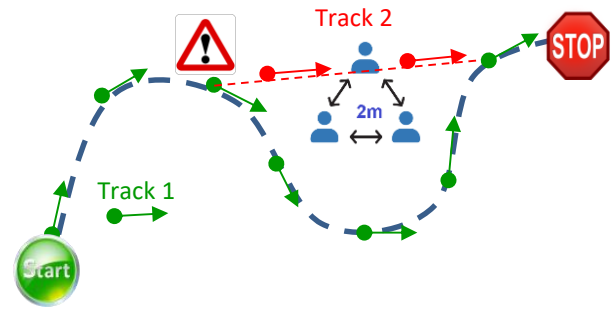


Figure 11 Safety close person virtual track.

The existence of congested zones can be locally detected by the “mesh / cellular” hybrid controller (Figure 1b), which is also equipped with a modem providing IP base connectivity to the central manager. The hybrid controller integrates the number of requests and individual positions, received during the same time interval. Once the individual positions are known, the relative positions are calculated. If the relative position is less than 2 m, a contamination risk locally exists and an alert message is send for the users and the CM is informed. This alert allows the CM to recalculate, in real time, the best route for the users that request wayfinding services avoiding crowded regions as exemplified in Figure 11.

V. CONCLUSIONS

A VLC multi-person cooperative localization dynamic LED-assisted navigation system for large indoor environments was proposed. For lighting, data transmission and positioning, white LEDs were used. A SiC optical MUX/DEMUX mobile receiver decodes the data and based on the synchronism and ID of the joint transmitters infers its location, point-to-point path, timing and user flows.

A VLC scenario was established and the communication protocol presented. Bidirectional communication between the infrastructures and the mobile receivers were analysed. Two cellular networks were tested and compared: square and hexagonal. Main results show that, for both topologies, the location of a mobile receiver, concomitant with data transmission is achieved. The LED-aided VLC navigation system makes possible to determine the position of a mobile

target inside the network, to infer the travel direction along the time and to interact with received information.

Minding the benefits of VLC, it is expected that this type of communication will have an important role in positioning applications. Moving towards real implementation, the performances of such systems still need to improve. As a future goal, we plan to finalize the embedded application, for experimenting in several network layouts. Effects as synchronization, shadowing and ambient light noise will be minimized by distributing lighting sources (MIMO techniques) to optimize the coverage.

#### ACKNOWLEDGEMENTS

The work was sponsored by FCT – Fundação para a Ciência e a Tecnologia, within the Research Unit CTS – Center of Technology and Systems, reference UIDB/00066/2020. The project IPL/IDI&CA/2020/Geo-Loc/ISEL, is also acknowledge.

#### REFERENCES

- [1] M. Vieira, M. A. Vieira, P. Louro, P. Vieira, and A. Fantoni “Wayfinding Services in Crowded Buildings Through Visible Light” The Sixth International Conference on Advances in Sensors, Actuators, Metering and Sensing, ALLSENSOR2021, Copyright: Copyright (c) IARIA, 2021, July 18, 2021, ISSN: 2519-836X, ISBN: 978-1-61208-875-4, pp. 1-8.
- [2] C. Yang and H. R. Shao, “WiFi-based indoor positioning,” *IEEE Commun. Mag.*, vol. 53, no. 3, pp. 150–157, Mar. 2015.
- [3] X. Y. Lin, T. W. Ho, C. C. Fang, Z. S. Yen, B.J. Yang, and F. Lai, “A mobile indoor positioning system based on iBeacon technology,” in *Proc. Int. Conf. IEEE Eng. Med. Biol. Soc.*, pp. 4970–4973, 2015.
- [4] C. H. Huang, L. H. Lee, C. C. Ho, L. L. Wu, and Z. H. Lai, “Real-time rfid indoor positioning system based on kalman filter drift removal and heron-bilateration location estimation,” *IEEE Trans. Instrum. Meas.*, vol. 64, no. 3, pp. 728–739, Mar. 2015.
- [5] N. U. Hassan, A. Naeem, M. A. Pasha, T. Jadoon, and C. Yuen, “Indoor positioning using visible led lights: A survey,” *ACM Comput. Surv.*, vol. 48, pp. 1–32, 2015.
- [6] E. Ozgur E. Dinc, O. B. Akan, “Communicate to illuminate: State-of-the-art and research challenges for visible light communications,” *Physical Communication* 17 pp. 72–85, 2015.
- [7] D. Tsonev, H. Chun, S. Rajbhandari, J. McKendry, S. Videv, E. Gu, M. Haji, S. Watson, A. Kelly, G. Faulkner, M., Dawson, H. Haas, and D. O’Brien, “A 3-Gb/s single-LED OFDM-based wireless VLC link using a Gallium Nitride  $\mu$ LED,” *IEEE Photon. Technol. Lett.* 26 (7), pp.637–640, 2014.
- [8] D. O’Brien, H. L. Minh, L. Zeng, G. Faulkner, K. Lee, D. Jung, Y. Oh, and E. T. Won, “Indoor visible light communications: challenges and prospects,” *Proc. SPIE* 7091, 709106, 2008.
- [9] M. Vieira, P. Louro, M. Fernandes, M. A. Vieira, A. Fantoni and J. Costa, “Three Transducers Embedded into One Single SiC Photodetector: LSP Direct Image Sensor, Optical Amplifier and Demux Device,” *Advances in Photodiodes InTech*, Chap. 19, pp. 403-425, 2011.
- [10] M. A. Vieira, P. Louro, M. Vieira, A. Fantoni, and A. Steiger-Garção, “Light-activated amplification in Si-C tandem devices: A capacitive active filter model,” *IEEE sensor journal*, 12, no. 6, pp. 1755-1762, 2012.
- [11] A. Jovicic, J. Li, and T. Richardson, “Visible light communication: opportunities, challenges and the path to market,” *Communications Magazine*, IEEE, vol. 51, no. 12, pp. 26–32, 2013.
- [12] S. B. Park, D. K.Jung, H. S. Shing, D. J. Shing, Y. J. Hyun, K. Li, and Y. J. Oh, “Information broadcasting system based on visible light signboard,” presented at *Wireless and Optical Communication 2007*, Montreal, Canada, 2007.
- [13] R. Rajesh, “Dynamic Vehicle and control” *Mechanical Engineering Series*, ISBN 978-1-4614-1433-9. 2012.
- [14] J. Ackermann, J. Guldner, W. Sienel, R. Steinhauser, and V. Utkin, “Linear and Nonlinear Controller Design for Robust Automatic Steering” *IEEE Transactions on Control Systems Technology* ( Volume: 3, Issue: 1, Mar 1995), pp. 132 – 143, DOI: 10.1109/87.3,70719, 1995.
- [15] A. Yousefpour, C. Kong, J. P. Jue, “All one needs to know about fog computing and related edge computing paradigms: A complete survey”, *Journal of Systems Architecture*, Volume 98, pp. 289-330, 2019.
- [16] M. Vieira, M. A. Vieira, P. Louro, P. Vieira, A. Fantoni, “Fine-grained indoor localization: optical sensing and detection,” *Proc. SPIE* 10680, *Optical Sensing and Detection V*, 106800H. 9 May 2018.
- [17] M. Vieira, M. A. Vieira, P. Louro, P. Vieira, A. Fantoni, “Light-emitting diodes aided indoor localization using visible light communication technology,” *Opt. Eng.* 57(8), 087105, 2018.
- [18] Y. Zhu, W. Liang, J. Zhang, and Y. Zhang, “Space-Collaborative Constellation Designs for MIMO Indoor Visible Light Communications,” *IEEE Photonics Technology Letters*, vol. 27, no. 15, pp. 1667–1670, 2015.
- [19] Y. Qiu, H-H. Chen and W-X. Meng, “Channel modeling for visible light communications—a survey”, *Wirel. Commun. Mob. Comput.* 2016; 16:2016–2034, 2016.
- [20] S. Imran Raza, S. Jabeen, R. Chaudhry, S. A. Hussain, A. Saeed, M. S. Bhatti and M. H. Raza, “Optical Wireless Channel Characterization For Indoor Visible Light Communications”, *Indian Journal of Science and Technology*, Vol 8 (22), DOI: 10.17485/ijst/2015/v8i22/70605, 2015.
- [21] H. T. Friis, “A note on a simple transmission formula” *Proc. IRE*34, pp. 254–256, 1946.
- [22] M. A. Vieira, M. Vieira, P. Louro, V. Silva, and P. Vieira, “Optical signal processing for indoor positioning using a-SiCH technology,” *Opt. Eng.* 55 (10), 107105, 2016.
- [23] M. Vieira, M. A. Vieira, P. Louro, and Vieira, “Positioning and advertising in large indoor environments using visible light communication,” *Opt. Eng.* 58(6), 066102, 2019.
- [24] C. Iddon, A. Hathaway and S. Fitzgerald, “CIBSE COVID-19 Ventilation Guidance”, *CIBSE*, 2020.